International Journal of Mechanical and Production Engineering Research and Development (IJMPERD)
ISSN(P): 2249–6890; ISSN(E): 2249–8001
Vol. 10, Issue 2, Apr 2020, 1187–1204

MODIFICATION OF OXIDATION BEHAVIOR OF Ni Ti SHAPE-MEMORY ALLOY BY YTTRIUM ADDITION

NAWAL MOHAMMED DAWOOD & OSAMAH IHSAN ALI

Department of Metallurgical Engineering, College of Materials Engineering, Babylon University, Babil, Iraq

ABSTRACT

The current research studies the influences of yttrium element as an addition on the behavior of oxidation of NiTi-Shape Memory Alloy system (SMAs). Specimens were manufactured by powder technology method, the blended powder consisting of titanium and nickel with constituents of (45 %wt.) and (55% wt.) correspondingly. Yttrium was added in different weight percentage of (0.5 and 0.9). The constituents of powders were blended for five hours and later compressed with stable compressing load of (800) MPa to cylinder-shaped specimens. Sintering procedure done at a specific temperature (950 °C for 6 hours) in vacuum circumstances ($10^{-4)}$ torr. Later, the specimens cool down in vacuum condition till room temperature. The outcomes of X-ray diffraction analysis revealed that entirely specimens (without and with additions) contained [NiTi (B19) and (NiTi (B2)]. Periodic oxidation tests were performed in static air at temperatures (800, 900, and 1000°C) for 100 hrs and 10 hours per period to evaluate the behavior of oxidation for all specimens. The results showed that the behavior of oxidation of NiTi (without and with additives) were subjected to parabolic law. Further, the performance of NiTi SMAs was modified after yttrium addition. For the base NiTi alloy, the parabolic rate constant (kP) differs from akP = $2.4502x10^{-7}$ (mg^2/cm^4)/s. at 800 °Cto a specific value of kP = $10.609x10^{-7}$ (mg^2/cm^4)/s. at 1000 °C, and the energy of activation (Q=297 kJ/mol), while NiTi 0.5 wt.% Y alloy, the (Kp) varies from a Kp = $0.531x10^{-7}$ (mg^2/cm^4)/s. at 800 °C to a value of Kp = $8.6x10^{-7}$ (mg^2/cm^4)/s.) at 1000 °Cand (Q= 187.6 kJ/mol), and for NiTi 0.9 wt.% Y, (kP) differs from a value of kP = $1.0780x10^{-7}$ (mg^2/cm^4)/s.) at 800 °Cto a value of kP = $7.2531x10^{-7}$ (mg^2/cm^4)/s. at 1000 °C. and Q =123.98 kJ/mol. The phases presents after periodic oxidation at 1000 °Cfor 100 hrs. and 10 hrs. per period of NiTi 0.9%Y SMA surface as revealed by XRD analysis are NiTi monoclinic, NiTi cubic, Ni_3Ti, and TiO_2

KEYWORDS: NiTi, Shape Memory Alloy, Oxidation, Yttrium & Activation Energy

Received: Mar 10, 2020; **Accepted**: Mar 30, 2020; **Published**: Apr 08, 2020; **Paper Id.**: IJMPERDAPR2020115

Original Article

1. INTRODUCTION

Nitinol has quickly become the most suitable material for selection for numerous implantation instruments, like self-expanding stents, according to its superelasticity characteristics. Though numerous research have confirmed decent resistant of corrosion as well as biocompatibility that Nitinol offers **[1-3],** current research have revealed that in certain suitcases Nitinol implants could be corroded in vivo and release of great content of nickel [4, 5]. It is accepted that the corrosion resistant of Nitinol alloy can be appropriately enhanced by modification of the surface like electro-polishing [1]. Electro-polishing of Nitinol creates a protector regular TiO_2 scale which defends the substrate metal from corroded environments. At high temperature air environments, Ti interact with oxygen gas to create a titanium oxide scale, besides the structure of TiO_2 scale is appropriate taking into consideration the bio-compatibility of materials. At the same time, many Nitinol implants have undergone many thermal periods to shape-set the apparatuses or adjust its temperatures of transformations as the last surface improvements techniques, in addition, it's appropriate to estimate the influences of Nitinol high temperature oxidation on its corrosion

resistance. Several authors [6-12] have inspected the influences of surface modifications on the surface constituents of NiTi; however, the oxidation mechanism at high temperature is not entirely realized.

NiTi-base Shape-Memory Alloys (SMAs) are the greatest significant SMAs owing to their greater qualities in the effect of shape-memory (SME), pseudoelasticity and capacity of damping **[13].** It is common that the adding of an additional element can affect the behavior of phase transformation and the mechanical -properties of binary NiTi alloys**[14]**. Ti50Ni50-xYx alloys have concerned much consideration in SMAs' demands in which the SMAs are typically manufactured to a plate form or wire. The manufacturing procedures of SMA plate or wire are hotrolled or wiredrawn, and both have manufactured the elevated temperature scales on the external surface. Accordingly, a comprehension of the elevated temperature scales consistence on the NiTi based SMAs is demanded, and the behavior of oxidation of NiTi SMA has been explored by some investigators **[15–19].** The apparent activation energy (Q) for the reaction of oxidation of Ni50Ti50 SMA is evaluated to be 226 kJ/mol, and the rate of oxidation exhibits a parabolic law **[17].** A multiple layered of oxide scale is consistence on Ti50Ni50 SMA, comprising of an outer TiO_2scale, a porous intermediate scale of the combination of Ni(Ti), TiO_2 and a thin inner $TiNi_3$scale**[17]**

Oxidation resistant progress by adding designated alloying elements [20], several investigators elaborated in this field and considered the consequence of the adding of alloying elements such as chromium, aluminum and copper into alloys of nitinol and how it effect the performance of nitinol SMAs in high temperatures and corrosive surroundings [21,22]. K. N. Lin et al. [21] examined the iso-thermal oxidation performance of Ti50Ni40Cu10 (SMA) in 700–1000 °C static air, Whereas, James and Smialek [23] investigated the behavior of oxidation of an elevated temperature shape memory alloys, Ni30Pt50Ti (at.%) by isothermal oxidation in static air for 100 hrs at limited temperature variety from 500 to 900 °C. In addition to that, Kim et al. [24] discovered the effect of hafnium addition on the oxidation behavior at elevated temperature and the oxide structure of Ti-49Ni-12Hf at elevated temperature (SMAs) shape memory alloys. In the current work, the effect of various Yttrium addition (0.5 and 0.9 wt%) was investigated. Though, owing to the best of our knowledge, the oxidation behavior and mechanism of NiTiY SMAs have not been systematically studied. In this study, NiTiY SMA was oxidized in elevated-temperature air. The oxidation mechanism and the activation energy are conversed and compared with those of binary NiTi.

2. EXPERIMENTAL WORK

2.1. Materials Used

Ni, Ti and Y powders were used in this work to manufacture specimens in this work.

2.1.1 Powders

The specifications of powders are existing in Table 1 with the purity percentage and average particle size (µm).

Table 1: Powders used to Make NiTi Specimens

Materials	Purity %	Average particle size (µm)
Titanium powder	99.86%	13
Nickel powder	99.21%	29
Yttrium powder	99.99%	8.5

2.1.2 Manufactured of Specimens

Powder metallurgy technique (P. M.) is used to manufacture specimens of nitinol SMAs. The procedure includes blending, compressing and sintering technique. Table 2 comprise constituents of the alloys that have used in the current work.

Table 2: The Constituents of the Manufactured Alloys in Weight Percentage

Alloys No.	Chemical Composition Weight Percentage
1	55 Ni - 45Ti
2	54.5 Ni - 45Ti – 0.5 Y
3	54.1 Ni - 45Ti –0.9 Y

2.1.3 Blending of Powders

Nickel and Titanium powders with Yttrium as modifiers were limited as to the required amounts. Wet blending was done using the electrical rolling blender instrument to obtain a uniform powders dispersion. Ceramic balls with different diameters had been used through the blending process to settle blending the powder for five hours. Ethyl alcohol had been supplemented to avoid friction between the powder particulates and the mold walls and to reduction the oxidation of particulates during blending procedure.

2.1.4 Powders Compressing

Steel die with Cylindrical shape was employed to manufacture the specimens by compressing pressure (800 MPa) was applied. The compacting pressure was done by (electric hydraulic press). Graphite as emollient was supplemented in a tiny amounts to minimize the friction between the die walls and particulates through compressing.

2.2 The procedure of Sintering

The green compressed specimens were subjected to sintering procedure using a tube oven with quartz pipe and vacuum pumps where it can get a vacuum atmosphere up to (10^{-4}) tor. The procedure was illustrated in Figure1. When the sintering procedure was completed, the specimens were kept in the oven to cool down up to room temperature.

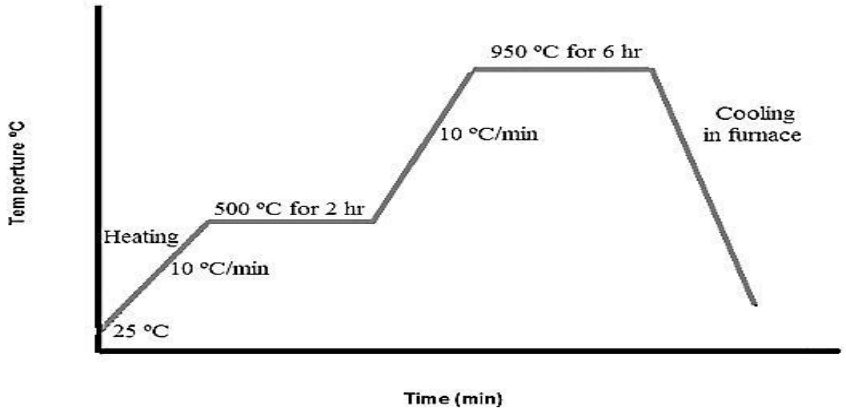

Figure 1: Sintering Procedure of Compressed Specimens.

2.3 Manufacturing of Specimens for Tests

All specimens after finishing sintering procedure were subjected to grinding using (180, 320, 600, 800, 1000,1200, and 2000) grit silicon carbide papers, then refined with a past of diamond (0.3 μm) to get a satin mirror surface for the last stage. The etching process was done using the following etching solution illustrated in Table 3, was done at 25 ℃. Later, the specimens were scavenge and rinsed by water and carefully dried.

Table 3: The Chemical Compositions and Concentrations of the used Etchant Solutions [25]

Chemical composition	Concentration of Etchant (%)
$HNO_3 + HF + H_2O$	20% + 10% + 70%

2.4. Measuring of Porosity and Density

Densities and porosities before and after sintering were determined according to the following sections.

2.4.1 Measuring of Green Porosity and Green Density

Green density can be defined as unit volume weight of compressed blended powder determined in grams per cubic centimeter. It is determined from measure of weight and dimensions of the compressed specimen as the following **[26]:**

$$\rho_g = \frac{m_g}{V_g} \quad (1)$$

Where:

ρ_g = green density (g/ cm³). , m_g = green mass of the compact (g).

V_g = volume of the compact (cm³).

The green porosity is calculated from theoretical density of blending that is considered by the weight percentage of elemental powders multiplies by their theoretical densities as the following **[26]:**

$$\rho_{tB} = \sum_{i=1}^{n} Wt_1 * \rho_1 + Wt_2 * \rho_2 + Wt_3 * \rho_3 + \ldots\ldots\ldots + Wt_n * \rho_n \quad (2)$$

Where:

ρ_{tB} = theoretical density of blended powder (g/cm³). , n = No. of elemental powders.

W_t = weight percent (%),

$\rho_{1,2,3,\ldots n}$ = density of elemental powder (g/ cm³).

So the green porositieswere calculated from the next equation **[26]:**

$$P_g = \left(1 - \frac{\rho_g}{\rho_{tB}}\right) \times 100\% \quad (3)$$

where

P_g = green porosity (%) . ρ_g = green density (g/ cm³).

ρ_{tB} = theoretical density of blended mixture (g/cm³).

True Porosities for Sintered specimens

2.4.2 Measuring of True Porosity for Sintered Specimens

Measuring of True Porosity for Sintered Specimens can be done according to ASTM B-328 as the following steps**[27]:**

- The specimens are dried at 100 ℃ for 5hrs. in vacuum condition at (10^{-4}) tor then cooled to R.T. by vacuum dryer oven. The weight of dry spacemen is symbolized as mass A.
- At R.T., by a sufficient vacuum pump. The pressure was reduced to the immersed specimen in suitable oil for 30 min
- Weighting the fully impregnated specimens in air, and is symbolized as mass B.
- Weighting the completely impregnated specimens in water, and is symbolized as mass F.
- Lastly, the porosity was calculated by the equation below:

$$P = \left[\frac{B-A}{(B-F)D^{\circ}} \times 100\right] Dw \quad (4)$$

Where:

D_w= water density (0.9956 g/cm3)

D_0 =oil density (0.8 g/cm3)

2.5 Inspection of Micro structure Using Scanning Electron Microscope (SEM)

The microstructures of the manufactured specimens were done after sintering procedure by Scanning Electron Microscope (SEM).

2.5.1 Periodic oxidation

Periodic oxidation at elevated temperature (800, 900, and 1000 ℃) were done to investigate the oxidation behavior and the influence of yttrium additive on oxidation performance evaluation of NiTi (SMAs). Through periodic oxidation, the temperature of oven was regulated by including $\pm$3℃. All NiTi alloys specimens without and with (0.5%, 0.9%) wt.% yttrium are tested. In each period, the specimens are pulled outside the oven to cool in the static air immediately after the heating period ends, and so the rest of the thermal periods are repeated until it reaches 100 hrs. Specimens weight recorded before and after each oxidation period.

2.6 X- Ray Diffraction Analysis

X-ray diffraction analysis was done for the powders of (nickel, titanium and yttrium) each one individually and specimens after sintering and after the end of periodicoxidation tests. The XRD generator with Cu target at 40 KV and 30 mA, scanning speed 5° per minute was performed. The scanning range was (10° – 90°).

3. RESULTS & DISCUSSIONS

3.1 Influence of Compacting Pressure and Sintering Procedure on Density and Porosity

Numerous values for compacting pressure (600,700 and 800) MPa were done in manufacturing the compressed specimens. Figure 2 shows the densities of Ni-Ti specimens with and without yttrium addition (0.5, 0.9) wt.%. When the compacting

pressure increased, the green density increased similarly till it extents a definite value where any additional growth in the applied pressure has no or small influence on its rate. Consequently the favored pressure was considered as 800 MPa for all the specimensmanufactured in the current work.

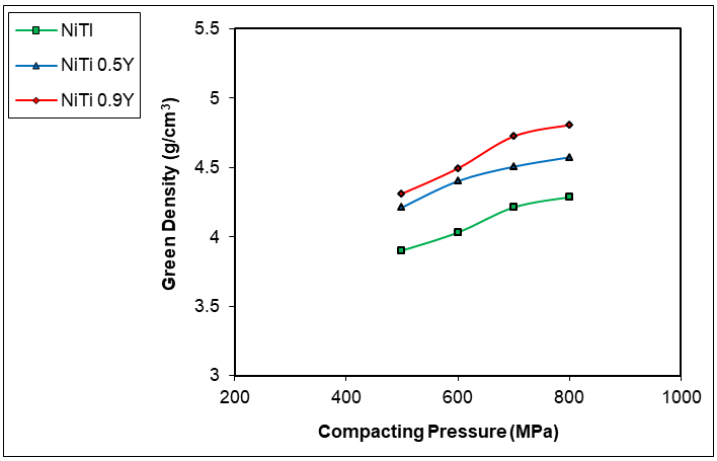

Figure 2: Green Density vs. Pressure before the Sintering Procedure of NiTi Alloy without and with Various Amounts of Yttrium.

The outcomes in Figure 3 display the specimens of NiTi with and without yttrium after sintering process. It illustrates that the density is increasing contineously as in Figure 2. This is attributed to the sintering procedure (950 ℃ for 6hr.s.) that cause increasing diffusion and reduction in voids. Since the particle size of the element yttrium is less than the particle size of nickel and titanium, this means an increase in contact points between blended powder particles, and as increasing yttrium content the density will increase, these results are in agreement and Nawalet. al.**[28]**

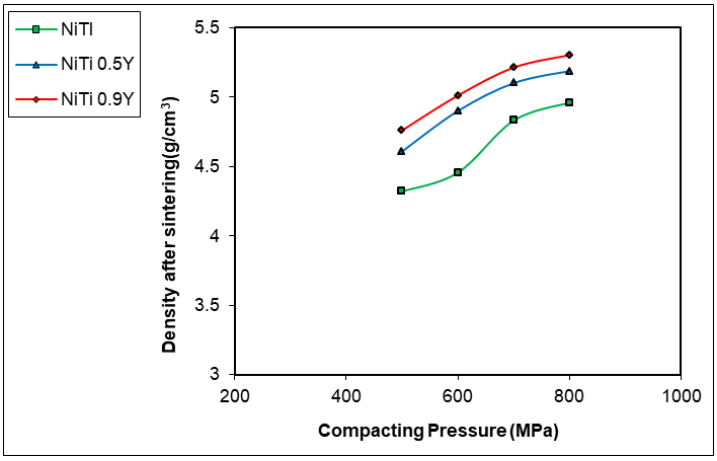

Figure 3: Density vs. Compacting Pressure after Sintering Procedure (at 950 ℃for 6hrs.) of NiTi Alloy with and without Yttrium.

Figure 4 shows that an increase in pressure of compacting give rise to a reduction in green porosity owing to the increase in the contact points between particulates that minimize voids.

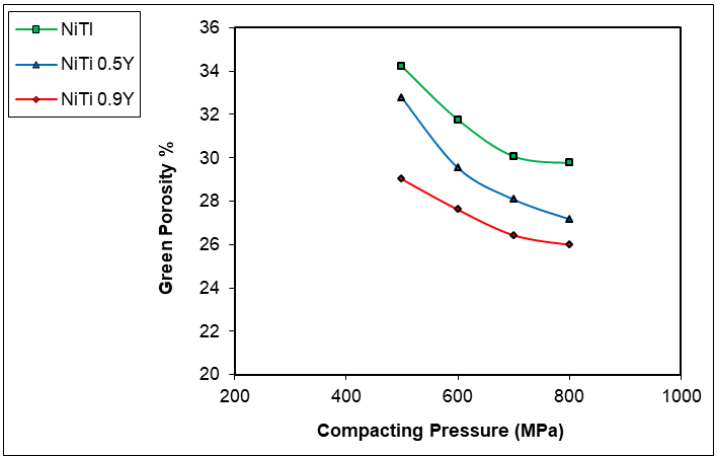

Figure 4: Green Porosity vs. Compacting Pressure before Sintering Procedure of NiTi Alloy without and with Yttrium.

The outcomes in Figure 5 display the porosity of specimens after sintering procedure. It demonstrates that the porosity has reduced owing to the sintering at 950 ℃ for 6hrs. increases diffusion between particles that reduces voids and increases the contact points between particles. This parameter will lead to less porosity.

3.2 Effects of Y Contents on Density and Porosity after Sintering:

Figure6 demonstrate the yttrium effect on porosity of sintered specimens, there is reduction in porosity values of specimens after sintering procedure. Porosity decreases with the increase of Y additions because the particle sizes of Y below than that of Ni or Ti, so when it occupies the interstitials positions, so the porosity decreases.

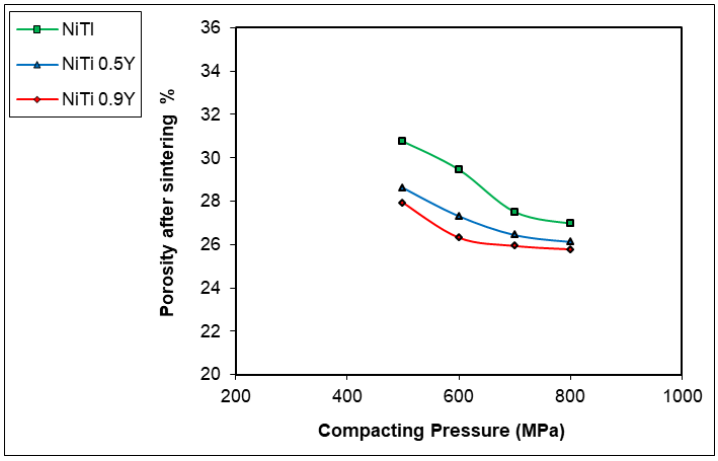

Figure 5: Porosity vs. Compacting Pressure after Sintering Procedure (at 950℃ for 6hrs.) of NiTi Alloy without and with Yttrium Amount.

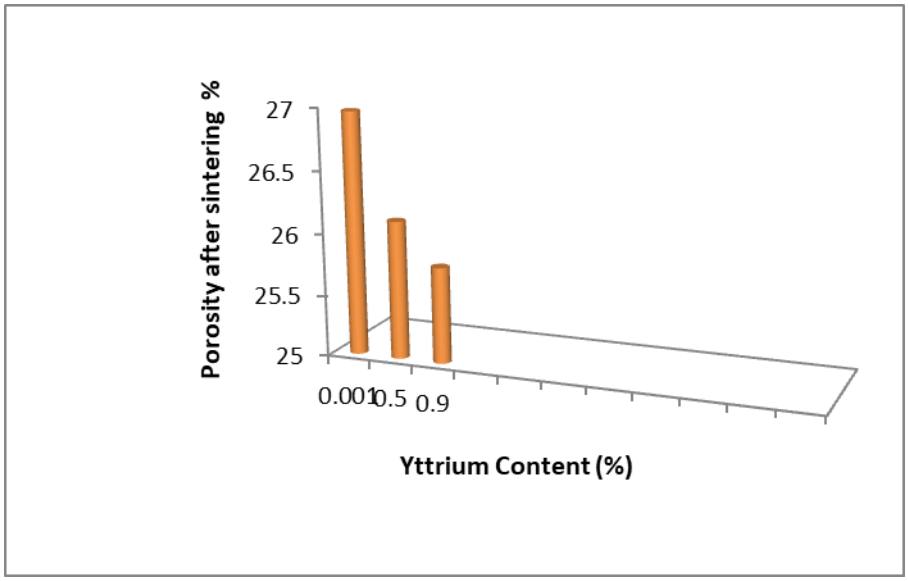

Figure 6: Influences of Yttrium amount on Porosity afterward Sintering Procedure for NiTi Alloy.

3.3 Scanning Electron Microscopy

The micro structures arrived from SEM for specimens without and with (0.9 wt.% Y) adding after being etched are revealed in Figures7 and 8 correspondingly. As an outcome, the microstructure of sintered specimen displayed a multi-phase construction whereas the two phases [B2 (NiTi Cubicphase) and B19' (NiTi monoclinic phase)], thus confirming XRD results.

It has been exposed from these Figures that the etching reveals grain boundaries, that easily distinguish with the boundaries of grains and pores form. The martensite shaped in entirely alloys has a needle formed grains. The order or dis-order of the parental phase B2 is converted to martensite, taking into consideration disorder B2 forms disordered martensite **[29].**

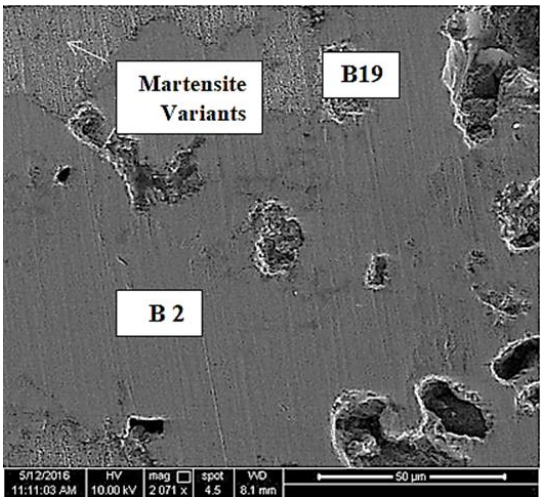

Figure 7: SEM of NiTi Alloy.

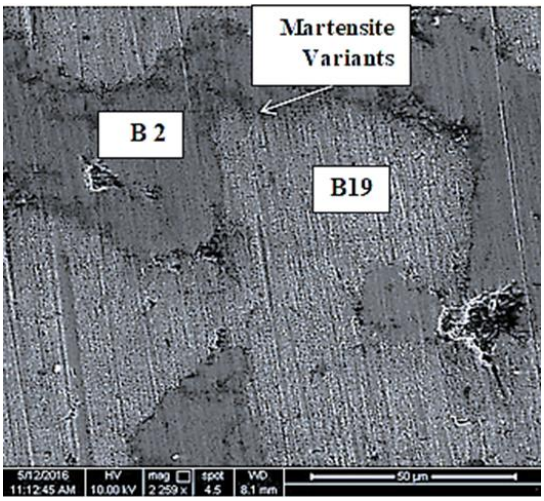

Figure 8: SEM of NiTi +0.9%Y Alloy.

3.4 Periodic Oxidation

This paragraph explains over the behavior of oxidation of NiTi (SMAs) and the influence of yttriumon these behaviors. NiTi specimen with chemical composition of (55% Ni,45% Ti) was examined to supply a typical to be associated with the periodic oxidation resistant of alloys that comprise of (0.5% and 0.9%) Yttrium. The function of Yttrium in modifying periodic oxidation resistant will be clarified. Gaining of weights were documented for kinetics definition in dried atmosphere in the temperatures variety 800 – 1000 °Cfor 100 hrs. and 10 hours per period. The data of specific weight gain of NiTi and alloys that comprise (0.5% and 0.9%) yttrium for every temperature test is schemed as a time function.

$$\Delta W/A = kt^{n} \quad (5)$$

Whereas (ΔW)is the gain of weight, (A) is the surface area of tested specimen, (k) is the rate constant, (n)is the growth- rate time constant, and (t)is the time of oxidation.

3.5 Oxidation of NiTi Alloy

In the state of NiTi alloy at 800 °C, the n-rate is around (0.49) i.e., the behavior is parabolic and it is found by (A computer database is employed to determine values of n by virtue of the best fit to Equation (5) Additional n values for entirely specimens and at different temperatures are revealed in Table4. Figure 9 presented Parabolic fitted outcomes of weight gain vs. time scheme for NiTi alloy periodic oxidized in dry air at temperatures among 800 and 1000 °C for 100 hrs. and 10 hours per period. These outcomes display that the parabolic kinetics at this temperature variety can be calculated on the improved parabolic rate law with the supposition that oxidation is measured by diffusion mechanisms and the boundaries of grains are the solitaryactive short circuit diffusion tracks [30].

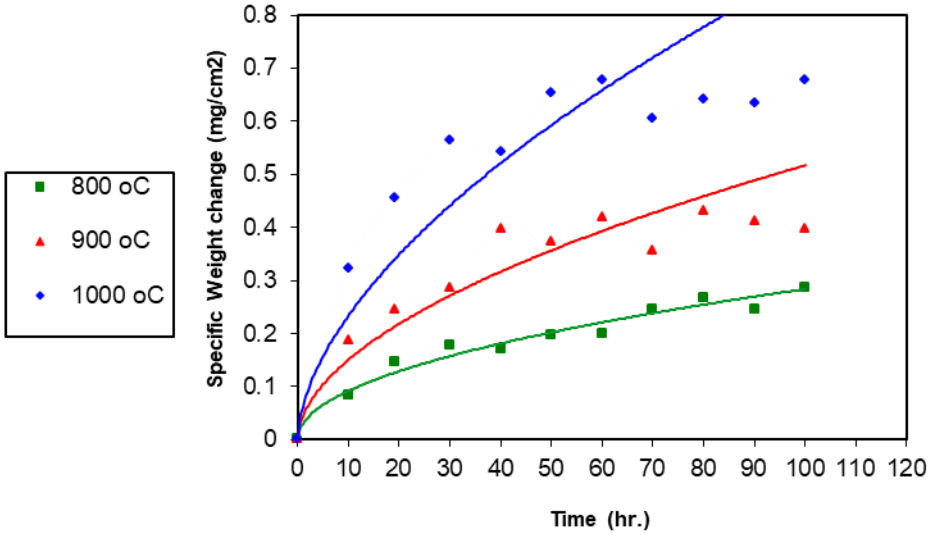

Figure 9: Parabolic Fitted Results of Specific Weight Gain vs. Time plot for NiTi Alloy Periodic Oxidized in air at Temperatures between 800 and 1000 ℃ for 100 hrs and 10 hours per Period.

For the parabolic kinetics, the rate equation receipts the formula:

$$\Delta W/A = kt^{0.5} \quad (6)$$

where k now denotes the parabolic rate constant. A scheme of the specific weight gain vs. square root of time provides a line as illustrated in Figure10; the sloping is the parabolic rate constant in units of $(mg/cm^2)/hr..^{1/2}$. The kP value is then squared to obtainkPin units of $(mg^2/cm^4)/hr..$, as in the subsequent expression:

$$(\Delta W/A)^2 = kPt \quad (7)$$

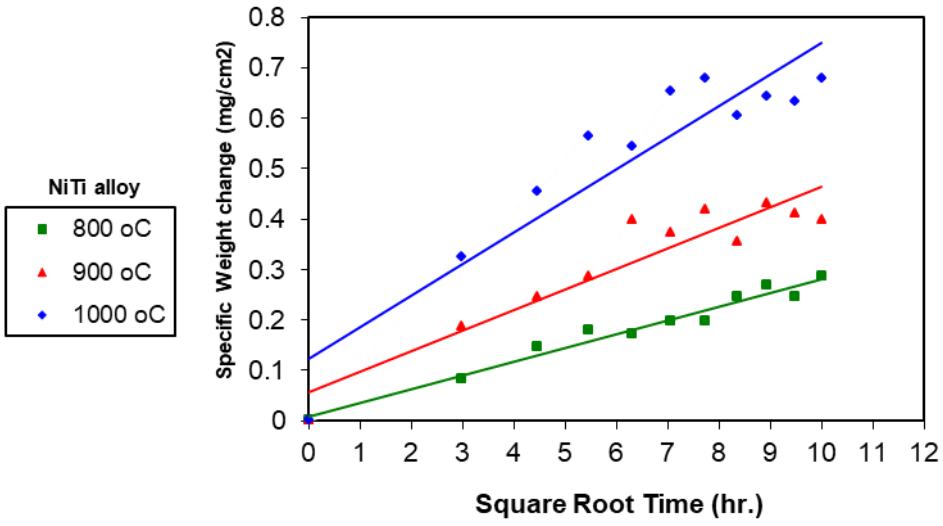

Figure 10: Linear Fitted outcomes of Specific Weight Gain vs. $t^{0.5}$ scheme for NiTi Alloy Periodic Oxidized in air at Temperatures among 800 and 1000 ℃for 100 hrs. and 10 hours per Period

The parabolic oxidation rate constants for three sequences of trials are determined and the linear lines indicate the least squares curve fits to the data values in Figure (11), the parabolic oxidation rate constants (kP) for the set of

experiments are itemized in Table (4).

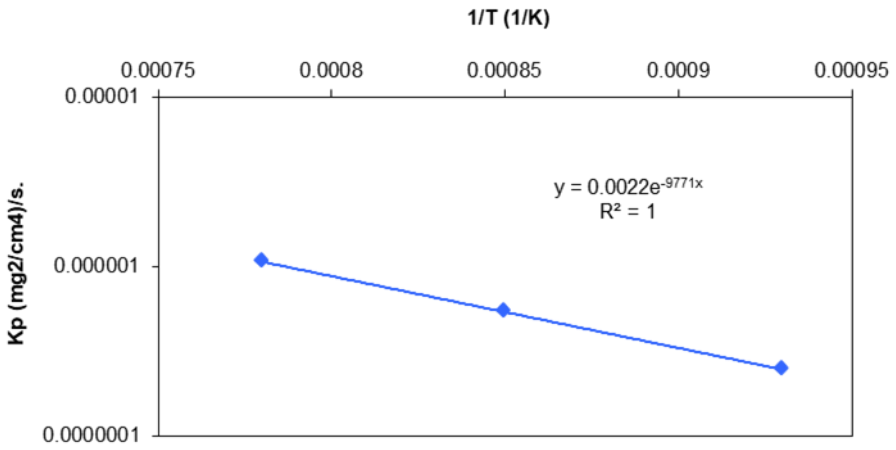

Figure 11: Scheme of kP vs. 1/T for NiTi Alloy Periodic Oxidized in Air for 100 hrs and 10 hours per Period.

Table 4: n Values and Parabolic Oxidation Rate Constants kP for Periodic Oxidation of NiTi alloy in air for 100 hrs. and 10 hours per Period

Temperature (°C)	n values	Kp (mg^2/cm^4)/s.
800	0.49	$2.4502 \boldsymbol{x}10^{-7}$
900	0.53	$5.3534 \boldsymbol{x}10^{-7}$
1000	0.57	$10.609 \boldsymbol{x}10^{-7}$

At the range of temperatures from 800 up to 1000 °C, the parabolic oxidation rate coefficients and accordingly the rates of oxidation of NiTi alloy in air, differ in amount from a little value of $2.4502\boldsymbol{x}10^{-7}(mg^2/cm^4)$/s. at 800 °C to a higher value of $10.609\boldsymbol{x}10^{-7}(mg^2/cm^4)$/s. at 1000 °C. The fact to be seen is that the weight gain determined by submission of the parabolic oxidation rates coefficient in Tableno 4 with Equation no. 3 produced in the weight of oxygen increased by the specimen underneath period icoxidation. Also, the insights to be seen, is that the additional values of n and kP in this investigation are determined with the similar method discussed above. From the investigational study, data exhibited that a parabolic oxidation rates (kP) submits an Arrhenius- type equations of the following:

$$k_P = k_o \exp(-Q/RT) \quad (8)$$

where kP is the rate of parabolic oxidation, k_o is the pre-exponential factor, Q is the energy of activation, T is the temperature, and R is the universal gas constant (8.33 J/K)[**31**]. Draw of log (kP) vs. (1/T), the operative energy is determined from the least square fitting ($R^2 = 1$) of the seen data in the temperature ranges from 800 to 1000 °C is to be ~ 297 KJ/mol. as illustrated in Figure11. The arrived value is in a good alignment with data from James L. Smialek **[23].**

3.6 Oxidation of (NiTi0.5Y) and (NiTi0.9Y) Alloy

It is to be noted from Figures 12 to 15 that the behavior of the two alloys (NiTi 0.5Y) and (NiTi 0.9Y) follows parabolic behavior when oxidized in a periodical manner in air for 100 hrs. and 10 hrs. per period and as it is noticed that the rise in temperature leads to an increase in weight as well.

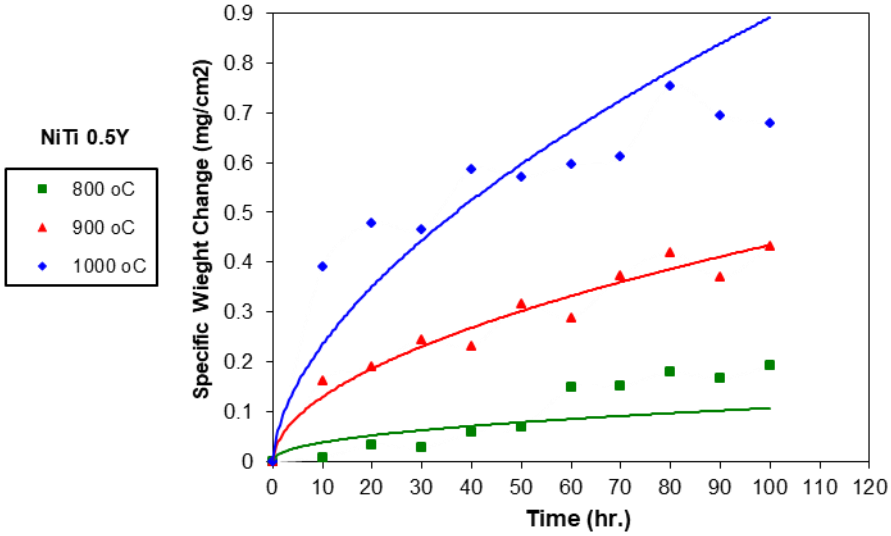

Figure 12: Parabolic Fitted Results of Specific Weight Gain vs. Time Scheme for NiTi 0.5%Y Alloy Periodic Oxidized in Air at Temperatures among 800 and 1000 ℃for 100 hrs. and 10 hrs. per Period.

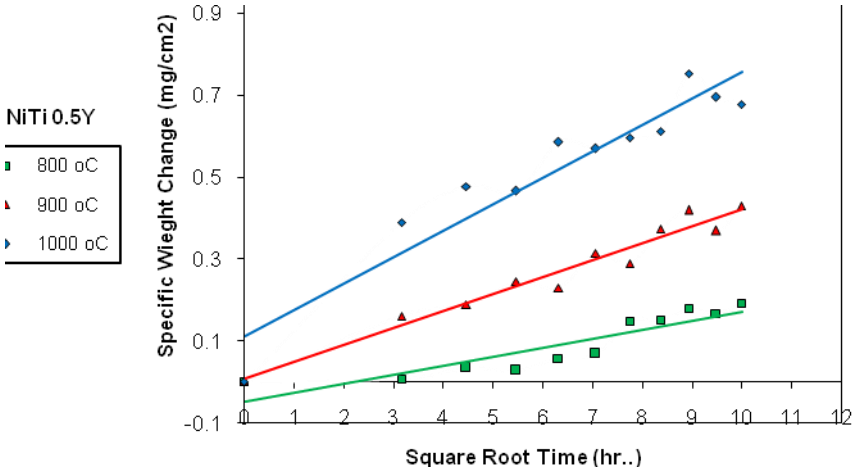

Figure 13: Linear Fitted Results of Specific Weight Gain vs. $t^{0.5}$ Scheme for NiTi 0.5Y Alloy Periodic Oxidized in Air at Temperatures among 800 and 1000 ℃ for 100 hrs. and 10 hrs. per Period

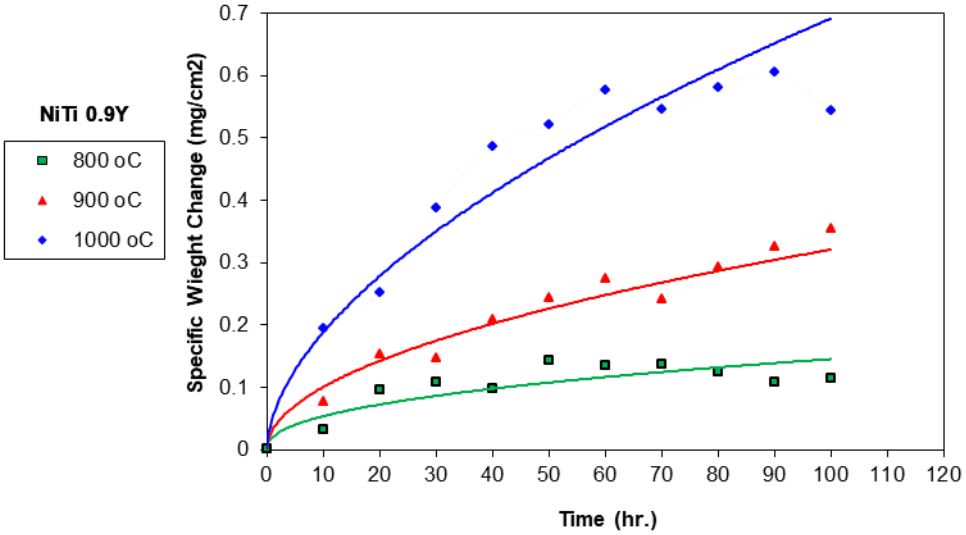

Figure 14: Parabolic Fitted Results of Specific Weight Gain vs. Time Scheme for NiTi 0.9%Y Alloy Periodic Oxidized in Air at Temperatures among 800 and 1000 ℃ for 100 hrs. and 10 hrs. per Period.

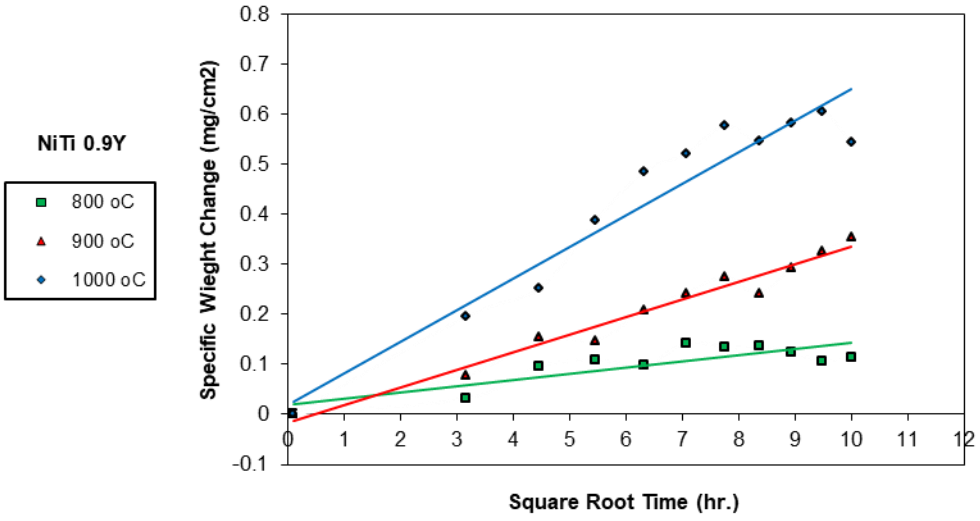

Figure 15: Linear Fitted Results of Specific Weight Gain vs. t0.5 Scheme for NiTi Alloy Periodic Oxidized in air at Temperatures among 800 and 1000 ℃for 100 hrs. and 10 hrs. per Period.

From the experimental data, the log of (kP) vs. (1/T) is schemed as shown in Figures16 and 17, (n, kp, and Q) revealed in Table 5 were determined from least square fitting of the recorded information in the range of temperature from 800 to 1000 ℃.

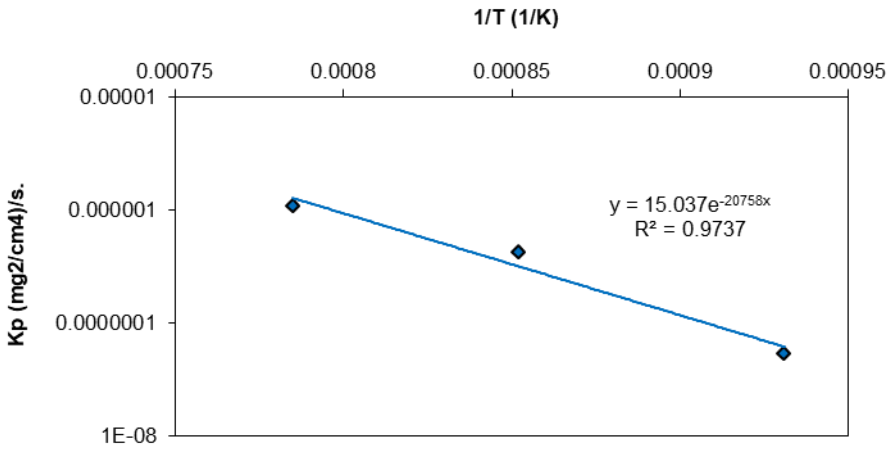

Figure 16: Scheme of kPvs. 1/T for NiTi 0.5 Y Alloy Periodic Oxidized in Air for 100 hrs. and 10 hrs. per Period

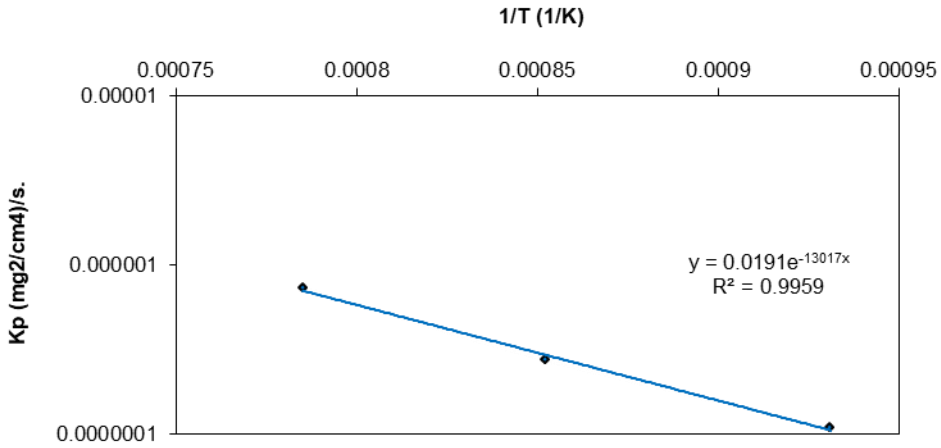

Figure 17: Scheme of kP vs. 1/T for NiTi 0.9 Alloy Periodic Oxidized in air for 100 hrs. and 10 Hours per Period.

Table 5: values of (n),(kP), and (Q)for (NiTi 0.5% Y) and (NiTi 0.9% Y) alloy periodic oxidized in air for 100 hrs. and 10 hours per period

alloy	Temperature (^{o}C)	n values	kP(mg^2/cm^4)/s.	Activation energy kJ/mol
NiTi 0.5% Y	800	0.443	$0.536x\ 10^{-7}$	187.6
	900	0.524	$4.185x\ 10^{-7}$	
	1000	0.577	$10.754x\ 10^{-7}$	
NiTi 0.9% Y	800	0.433	$1.078x\ 10^{-7}$	123.95
	900	0.5053	$2.721x\ 10^{-7}$	
	1000	0.5657	$7.253x\ 10^{-7}$	

From the outcome, it is established that weight gain affected by the quantity of yttrium additional to the alloy. At 800°C, weight gain of alloy that comprises(0.9%Y) is lesser than the others, therefore, the resistance of oxidation is the

maximum since the oxide scale thickness is lesser. Which means that oxide scale create on the surface of metal could stop more reactions with oxygen at(900and 1000)℃ oxidation resistant is the upper most at(0.9%Y).

3.7 X- Ray Diffraction Tests

Figures 18 demonstrate the XRD configuration for NiTi with the addition of 0.9Y afterward sintering procedure. It can be realized that Ni and Ti converted to (B19 martensite and B2 austenite). This illustrates that the sintering procedure time (6 hrs. at 950 ℃) was sufficient to complete the phases alteration procedures. The non appearance of pure elements are important in the X-ray diffraction analysis is very important. If we take into account the toxicity caused due to some pure elements biomaterials applications. Yttrium compounds have not been clearly demonstrated in the X-ray diagrams, and this is due to the low-level added yttrium (0.9), which is outside the limits of the possible detection ranges.

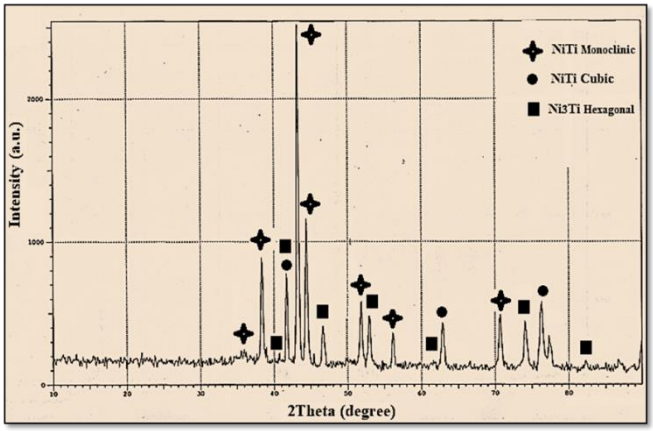

Figure 18: XRD Configuration for NiTi0.9%Yalloy afterward Sintering Procedure.

Figure19 demonstrates XRD configurations of NiTi 0.9%Y alloy after subjected to periodic oxidation at 1000 ℃. Oxides are created on the specimen surface. The main constituent of these oxides is titanium oxide. That means that TiO_2 development controls the oxidation behavior. This is due to the action of yttrium or yttrium compounds phases which may be found on the outer scale in smallamounts [32].

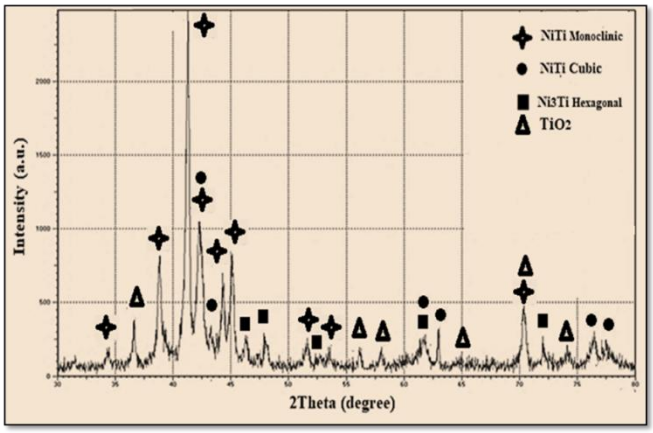

Figure 14: XRD Configurations of NiTi 0.9%Y SMA after Periodic Oxidized for 100 hrs and 10 hours per Period at 1000 °C.

4. CONCLUSIONS

- Procedure of sintering procedure at 950 ℃ for six hours (with and without yttrium addition) is sufficient to fulfillment the process of transformation of nickel, titanium and yttrium to alloy construction.

- The results of scanning electron microscopy showed that the main phase formed for all specimens without and with the addition of yttrium the martensite phase.
- The porosity decreases significantly with the addition of yttrium.
- The X-ray examination results indicated formation of austenite (B2) and monoclinic NiTi (B19) for all specimens.
- The NiTi alloy showed good periodic oxidation resistance at temperatures 800 ℃, 900℃ and 1000 ℃.
- NiTi alloy exhibited sufficient periodic oxidation resistance at 800 ℃, 900℃ and 1000 ℃.
- The addition of yttrium to the NiTi alloy greatly improved the oxidation resistance in general, and the addition 0.9 wt.% Y gave the best results in particular.
- All NiTi alloys (with and without additives) showed parabolic oxidation behavior in all conditions
- The activation energy of NiTi is ~ 297 kJ/mol,(NiTi0.5%Y)~ 187.6 kJ/mol and that for (NiTi0.9%Y) ~ 123.95 kJ/mol. This is a very clear indication of the low activation energy to form a protective layer of titanium oxide with the addition of yttrium to the nickel titanium alloy.

REFERENCES

1. *L. Zhu, C. Trépanier, A. R. Pelton and J. Fino, Oxidation of Nitinol and its Effect on Corrosion Resistance, ASM Materials & Processes for Medical Device Conference,2003.*
2. *G. S. Firstov*, R. G. Vitchev1, H. Kumar, B. Blanpain, J. Van Humbeeck, Surface oxidation of NiTi shape memory alloy, Biomaterials 23 (2002) 4863–4871.*
3. *Abdus Mahmuda, b, Zhigang Wua, c,**, Junsong Zhanga, Yinong Liua,*, Hong Yanga, Surface oxidation of NiTi and its effects on thermal and mechanical properties, Intermetallics103(2018)52–62.*
4. *A. Michiardi, C. Aparicio, J. A. Planell, F. J. Gil, New Oxidation Treatment of NiTi Shape Memory Alloys to Obtain Ni-Free Surfaces and to Improve Biocompatibility, MICHIARDI ET, AL Wiley InterScience (www.interscience.wiley.com). DOI: 10.1002/jbm.b.30441, 2005, pp.249-256.*
5. *N. M. Dawood, A. K. Abid Ali, and A. A. Atiyah, Fabrication of Porous NiTi Shape Memory Alloy Objects by Powder Metallurgy for Biomedical Applications, IOP Conf. Series: Materials Science and Engineering, 518 (2019) 032056, doi:10.1088/1757-899X/518/3/032056*
6. *M. Duerig and P. Sinclair, Two-Step Martensitic Transformations in TiNi (10% Cu) Shape Memory Alloy, Materials Research Society Symposium Proceedings Vol. 245 "Shape Memory Materials and Phenomena - Fundamental Aspects and Applications" 1992, pp. 55-60*
7. *Z. Yang, X. Wei, P. Caoand W. Gao, Surface Modification of Nitinol by Chemical and Electrochemical Etching, Modern Physics Letters B, Vol. 27, No. 19, (2013) 1341012 (7 pages).*
8. *F. Sun , K. Sask, J. Brash, I. Zhitomirsky, Surface Modifications of Nitinol for Biomedical Applications. Colloids Surf B Bio interfaces. 2008 Nov 15;67(1):132-9. doi: 10.1016/j.colsurfb.2008.08.008. Epub 2008 Aug 22.*
9. *Z. Yang, X. Wel, P. Cao and W. Gao, Surface Modification of Nitinol by Chemical and Electrochemical Etching, Modern Physics Letters B, Vol. 27, No. 19, 1341012 (2013)*
10. *O. A. Kashin, D. P. Borisov, A. I. Lotkov, P. V. Abramova, and A. V. Korshunov, Influence of surface modification of nitinol*

with silicon using plasma-immersion ion implantation on the alloy corrosion resistance in artificial physiological solutions, AIP Conference Proceedings 1683, 020077 (2015); https://doi.org/10.1063/1.4932767S. Trigwell, et al., in Sufr Interface Anal, 26, 1998, p. 483-489.

11. *S. Shabalovskaya, J. Anderegg, J. Van Humbeeck, Critical overview of Nitinol surfaces and their modifications for medical applications, ActaBiomaterialia 4 (2008) 447–467.*
12. *A F Mansor, R Jamaluddin, A I Azmi, T C Lih and M Z M Zain, Surface modification of nitinol by using electrical discharge coatings in deionized water, IOP Conf. Series: Materials Science and Engineering 670 (2019) 012010, doi:10.1088/1757-899X/670/1/012010C.*
13. *Xiangmei Liu, Shuilin Wu, Y. L. Chan, Paul K. Chu, C. Y. Chung, C. L. Chu, K. W. K. Yeung, W. W. Lu, K. M. C. Cheung, K. D. K. Luk, Structure and wear properties of NiTi modified by nitrogen plasma immersion ion implantation, Materials Science and Engineering A 444 (2007) 192–197*
14. *Xiangqing Kong, R. G. Grabitz, W. van Oeveren, D. Klee, T. G. van Kooten, F. Freudenthal, Ma Qing, G. von Bernuth, M.-C. Seghaye, Effect of biologically active coating on biocompatibility of Nitinol devices designed for the closure of intra-atrial communications, Biomaterials 23 (2002) 1775–1783*
15. *F. S. Hameed and A. H. Haleem, Investigation the Effects of Germanium addition on the Oxidation Behavior of NiTi shape memory Alloy in Air, ADVANCES in NATURAL and APPLIED SCIENCES, 2017 January 11(1): pp. 31-44.*
16. *Edin Bazochaharbakhsh, Surface Nitriding and Oxidation of Nitinol, Master's Theses, San Jose State University, August 2011.*
17. *S. A. Shabalovskaya, H. Tian, J. W. Anderegg, D. U. Schryvers, W. U. Carroll and J. V. Humbeeck, "The Influence of Surface Oxides on the Distribution and Release of Nickel From Nitinol Wires," Biomaterials, 30, 468-477, (2009).*
18. *G. S. Firstov, R. G. Vitchev, H. Kumar, B. Blanpain and J. Van Humbeeck, "Surface Oxidation of NiTi Shape Memory Alloy," Biomaterials, 23(24), 4863-4871(2002).*
19. *L. Zhu, J. M. Fino and A. R. Pelton, "Oxidation of Nitinol," in International Conference on Shape Memory and Superelastic Technologies, USA, 2003, pp. 357–368, (2003).*
20. *D. Mudgal, S. Singh and S. Prakash, "High Temperature Periodic Oxidation Behavior of Ni and Co Based Super alloys", Journal of Minerals & Materials Characterization & Engineering, Vol. 11, No.3, pp.211-219, (2012).*
21. *K. Lin and Sh. Wu, "Oxidation Behavior of Ti50Ni40Cu10 Shape-Memory Alloy in 700–1,000 _C Air", Oxid. Met, Taiwan, P. 187–200 (2009).*
22. *C. Craciunescu and A. S. Hamdy, "The Effect of Copper Alloying Element on the Corrosion Characteristics of Ti-Ni and Ternary Ni-Ti-Cu Meltspun Shape Memory Alloy Ribbons in 0.9% NaCl Solution", Int. J. Electr°Chem. Sci, Egypt No.8, P. 10320 - 10334 (2013).*
23. *J. L. Smialek, D. L. Humphrey and R. D. Noebe, "Comparative oxidation kinetics of a NiPtTi high temperature shape memory alloy", Oxidation of metals, P. 125-144. (2010).*
24. *K. M. Kim, J. T. Yeom, H. S. Lee, S. Y. Yoon and J. H. Kim, "High temperature oxidation behavior of Ti–Ni–Hf shape memory alloy". Therm°ChimicaActa, 583, 1-7. (2014).*
25. *P. Walker and W. H Tarn, "CRC handbook of metal etchants", CRC press, (1990).*
26. *S. A. Ajeel, A. K. A. Ali and M. A. Alher, "Ni Ion Release of TiO2 and TiO2/Hydroxylapatite composite coatings formed on NiTi shape memoryalloy produced by powder metallurgy". International Journal of Mechanical Engineering and Technology, P. 86-99, (2013).*

27. *ASTM B-328" Standard Test Method for Density, Oil Content, and Interconnected Porosity of Sintered Metal Structural Part and Oil – Impregnated Bearing "ASTM international, 2003*

28. *Atiyah, A. K. Abid Ali, N. M. Dawood, Characterization of NiTi and NiTiCu Porous Shape Memory Alloys Prepared by Powder Metallurgy (Part I), Arabian Journal for Science and Engineering, 40, pp.901–913(2015)*

29. *N. M. Dawood, " Preparation And Characterization Of Bio Nitinol With Addition Of Copper", PhD. thesis, materials engineering department, university of technology/ Iraq, 2014.*

30. *Michiardi, C. Aparicio, J. A. Planell and F. J. Gil, "New Oxidation Treatment of NiTi Shape Memory Alloys to Obtain Ni-free Surfaces and to Improve Biocompatibility," J. Biomed. Mater. Res., 77, pp.249-256, 2006.*

31. *D. Vojtech, P. Novak, M. Novak, L. Joska, T. Fabian, J. Maixner and V. Machovic, "Cyclic and Isothermal Oxidations of Nitinol Wire at Moderate Temperatures," Intermetallics, 16, 424-31, (2008).*

32. *A. H. Khilfa"Effect of Y and Ge addition on Mechanical properties and Corrosion Behavior of Biomedical C°CrMoAlloy (F75)", master thesis, Materials engineering, University of Babylon, (2015).*